Tribology International 150 (2020) 106370

Contents lists available at ScienceDirect

Tribology International

journal homepage: http://www.elsevier.com/locate/triboint

Study on the polishing mechanism of pH-dependent tribochemical removal in CMP of CaF_2 crystal

Jie Guo, Jian Gong, Pengfei Shi, Chen Xiao, Liang Jiang, Lei Chen *, Linmao Qian

Tribology Research Institute, State Key Laboratory of Traction Power, School of Mechanical Engineering, Southwest Jiaotong University, Chengdu, 610031, China

ARTICLE INFO

Keywords:
Atomic material removal
pH-dependent tribochemistry
CMP
CaF_2

ABSTRACT

Nanowear tests of calcium fluoride (CaF_2) crystal against SiO_2 microspherical tip at various pH solutions were conducted using an atomic force microscope to detect the atomic removal mechanism in chemical mechanical polishing (CMP). An optimized solution pH range was defined as 9–10, below which the atomic material removal of CaF_2 cannot occur and above which the excessive chemical corrosion pits will form at the fabricated surface. TEM analysis of wear track demonstrates no remarkable subsurface damage in the wear region, confirming the domination of tribochemical reactions. Finally, the optimized pH was applied in real CMP and the ultimate limit of tribochemical wear in CMP was determined, i.e., a removal of $Ca–F^+$ layer from a $CaF_2(111)$ cleavage surface.

1. Introduction

As a key material used in high-power laser optics, single-crystal calcium fluoride (CaF_2) requires extremely high surface accuracy, such as sub-nano roughness and nearly defect-free surface [1–3]. Chemical mechanical polishing (CMP) has been applied successfully to fabricate atomic-level smooth-surfaced semiconductor [4,5] with great potential for the ultraprecision manufacturing of CaF_2 surface [6,7]. In CMP, slurry chemistry is typically optimized to enhance a chemical reaction, which can facilitate material removal and minimize residual subsurface damage [8,9]. By adjusting pH of the CMP slurry, polishing parameters, polishing particle size and surface chemistry, etc., the roughness of polished CaF_2 surface can be reduced to sub-nanometer level [10]. Although the role of slurry pH is significant, the mechanism of the pH-dependent material removal of CaF_2 remains unclear, thereby partial responsible for hindering further improvement of the surface quality of CaF_2 CMP.

The practical CMP process relates to a complicated material removal mechanism involving mechanical interaction, tribochemical reaction, or even corrosion in particles, solutions, and substrate systems [11,12]. Therefore, in addition to the practical process parameters, such as applied load and plate speed [13], the properties of polishing slurry (i.e., flow rate, nanoparticle concentration, and chemistry) may simultaneously influence the polished surface quality [8–10,14]. Although exactly the same single-abrasive-contact in CMP is difficult to be simulated experimentally due to its complex motion, such as scratch, rolling and turning, the single-point contact wear model, such as that in atomic force microscope (AFM) tests, provides a new perspective for qualifying the effect mechanism of these parameters due to the main domination of mechanochemical reaction of material removal in CMP, which is independence of motion form. For instance, decrease in sliding speed (or increase in contact time) and increase in mechanical stress or temperature can facilitate a tribochemical reaction, resulting in great atomic material removal [15–17]. Furthermore, water molecules play a critical role in tribochemical wear [18–20]. In dry air, the surface damage of crystal CaF_2 undergoes transition from plastic deformation (plane slipping) to brittle removal (crack propagation) with increase of the applied load [21]. Under liquid conditions, a tribochemical reaction causes the atomic layer removal of fresh CaF_2 cleavage surface at the contact pressure even below the yield stress [22]. Mechanical damage, such as plane slipping or delamination, can be suppressed in water at high mechanical stress [23,24]. Even so, previous works normally focused on the effect of water on the material removal mechanism of CaF_2, but the solution pH should be given more attention because it determines the initiation of tribochemical reaction in CaF_2 CMP.

In this study, we present the effect of solution pH on the atomic material removal of $CaF_2(111)$ surface rubbed against a SiO_2 single abrasive. The tribochemical wear mechanism of CaF_2 was detected in deep by analyzing the friction and adhesion behaviors combining with high resolution transmission electron microscope (TEM) characterizations. The tribochemical wear of $CaF_2(111)$ surface was found to occur without residual surface corrosion wear and subsurface lattice damage

* Corresponding author.
E-mail address: chenlei@swjtu.edu.cn (L. Chen).

https://doi.org/10.1016/j.triboint.2020.106370
Received 5 November 2019; Received in revised form 4 April 2020; Accepted 10 April 2020
Available online 21 April 2020

at pH of 9–10. Under the optimized pH conditions, the ultimate limit in CMP was determined, that is, removal of Ca–F^+ layer from CaF_2(111) cleavage surface, and a sub-nano rough surface can be produced in CMP. This study bridges single abrasive sliding tests and actual CMP by detecting the role of solution pH in atomic material removal, which may shed new light on the tribochemical wear mechanism of CaF_2 in CMP.

2. Experimental methods

The samples used in reciprocated sliding wear tests were polished CaF_2(111) wafers with a root-mean-square (RMS) roughness of 0.52 ± 0.24 nm over a 5 × 5 μm^2 area. The samples used in the atomic layer removal tests and CMP were CaF_2(111) cleavage surfaces prepared by razor blade cleaving. To remove possible adsorbed contaminants, each sample was ultrasonically cleaned in ethanol for ~3 min, washed with deionized (DI) water, and dried in pure nitrogen before wear or CMP tests.

To simulate the single-abrasive-contact state in CMP, reciprocated sliding and area-scanning wear tests of CaF_2(111) surface slid against a SiO_2 microspherical tip (radius ≈ 1.25 μm) were performed using an AFM (SPI3800 N, Seiko, Japan) and a liquid cell for solution pH control (Fig. 1a). The solution pH that was determined using an ultra-precision pH meter (mp512-02, Shanghai Sanxin instrument factory, China) ranged from 6 to 12 through regulating the concentration of KOH dissolved in DI water. The well-prepared KOH solutions were used in nanowear tests immediately to ensure the pH accuracy. Using a calibration probe with a force constant of 2.957 N/m, the normal spring constants of the cantilevers of SiO_2 AFM tips were calibrated as 10.5–13.8 N/m [25]. If not specified, the wear tests were performed under room temperature, the applied normal load F_n was 4.9 μN, the sliding speed v was 8 μm/s, and the number of sliding cycles was 200. After the wear tests, the worn surfaces were imaged using a sensitive Si_3N_4 tip (MLCT, Veeco, USA) with a nominal curvature radius of ~12 nm and a nominal spring constant of 0.1 N/m. The wear volume was calculated based on the average cross-section area of the wear scar times the sliding displacement. A selected set of wear scar on the CaF_2 substrate was analyzed using TEM (Tecnai G2, FEI, USA). The cross-section sample was prepared using a focused ion beam system (Nanolab Helios 400S, FEI, Holland). To verify the optimized solution pH obtained from the AFM tests, the actual CMP of a CaF_2(111) cleavage surface was carried out sequentially using a polisher (UNIPOL-802, MTI, USA) with diamond and silica polishing slurries (Fig. 1b). Table 1 presents the polishing parameters. Each polished CaF_2 surface was ultrasonically cleaned with DI water and imaged using AFM with the sensitive Si_3N_4 tip.

3. Results and discussion

3.1. 1 pH dependence of atomic removal on CaF_2 surface

Fig. 2a demonstrates the morphologies of CaF_2 surface after the sliding wear tests in pure water at pH = 6 and in KOH solutions at pH = 9–12. As the pH level of the solution increases from 6 to 12, the surface wear of CaF_2 transforms from having no visible surface damage to obvious material removal at a critical pH of ~9. When the atomic material removal of CaF_2 occurs at pH > 9, the wear depth increases from ~1.4 nm at pH = 10 to ~2.5 nm at pH ≥ 11. Fig. 2b plots the entire wear volume data measured in the range of pH. As solution pH increases, the wear volume of CaF_2 increases gradually at pH ≤ 9 and almost levels off when the pH increases from 11 to 12.

Under the given normal load of 4.9 μN and with maximum adhesion force of approximately 0.45 μN, the contact pressure between the CaF_2/SiO_2 interface is estimated at ~1.13 GPa based on Derjaguin–Muller–Toporov model. Here, the elastic modulus applied at the CaF_2 surface is 115 ± 15 GPa [10]. At the CaF_2(111) surface, the maximum contact stress corresponding to the material yield limit under scratch was detected at approximately 10.8 GPa [10], which is considerably larger than the value applied in this study. Hence, mechanical interaction alone cannot reasonably activate the surface wear of CaF_2 under the given AFM experimental conditions; this phenomenon is supported by the wearlessness of CaF_2 at pH = 6 and 9. Therefore, atomic material removal at pH > 9 may be attributed to the tribochemical reaction under chemical solution etching.

Chemical etching can facilitate surface wear, but an extremely strong chemical reaction may result in surface defects [26]. Here, the effect of solution pH on the surface quality after material removal is assessed by using area-scanning model in AFM tests (Fig. 3a). The number of sliding lines in a scanning area of 1.5 × 1.5 μm^2 is 512, and then the scanning interval can be calculated as ~2.93 nm. Given that no visible surface wear is characterized below pH = 9, Fig. 3 demonstrates only the topographies of CaF_2 surfaces after area scanning in KOH solutions at pH = 10 and 11. When the solution pH is 10, material removal can be observed in the scanning region with a small wear depth, as the cross-section profile (black line) shown in Fig. 3b. As the pH increases to 11, more materials are removed under the same scanning conditions, and the wear depth increases to ~1.1 nm (cross-section profile in Fig. 3d). However, tiny and dense corrosion pits can be observed on the scanned surface (Fig. 3e). This finding may be due to the chemical corrosion of strong alkaline solution [4], which seems to be absent in pH 10 (Fig. 3c). The results in Figs. 2 and 3 show that although the strong basic solution is conducive to the material removal of CaF_2, the chemical corrosion of KOH solution on the surface of CaF_2 is intensive, resulting in excessive chemical corrosion damage on the surface, which reduces the quality of the processing surface. Here, the AFM tests indicate that the optimal pH of the polishing slurry for the CMP of CaF_2 surface is approximately 9–10.

3.2. Interfacial interaction between CaF_2/SiO_2 contacting surfaces at different pHs

Fig. 4 shows the variation in the friction force with the number of sliding cycles under different solution pH conditions. The friction forces decrease slightly as the pH increases from 6 to 9 and then increases to a maximum value of pH = 10 following the decrease with further increase

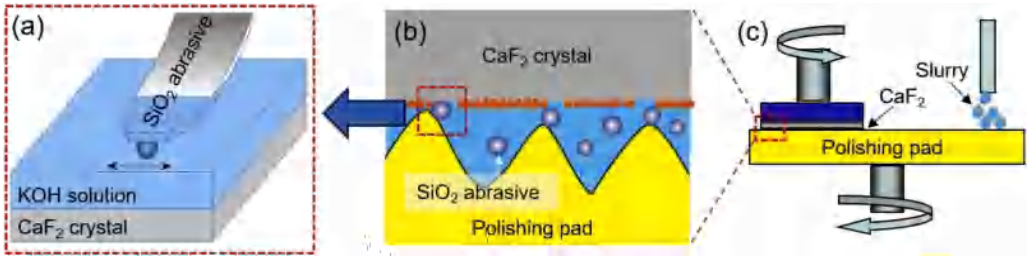

Fig. 1. Schematic illustration of a SiO_2 microspherical tip sliding against CaF_2 in AFM tests (a) to simulate single abrasive contact in actual CMP process (b) In the AFM tests, the SiO_2 microsphere with a radius of ~1.25 μm moved horizontally on the CaF_2 wafer under water or KOH solutions. In an actual CMP process, the pH of the polishing slurry was controlled according to the optimized value obtained in the AFM tests.

Table 1
CMP parameters for polishing the CaF_2(111) cleavage surface.

Slurry abrasive	pH of slurry	Polishing pad	Polishing pressure (kPa)	Rotation speed (r/min)	Velocity of fluid flow (ml/min)
Diamond nanoparticle	9.5–10	Non-woven fabrics	40 ± 10	600	100–150
Silica nanoparticle	9.5–10	Flexurane	44 ± 1	120	50

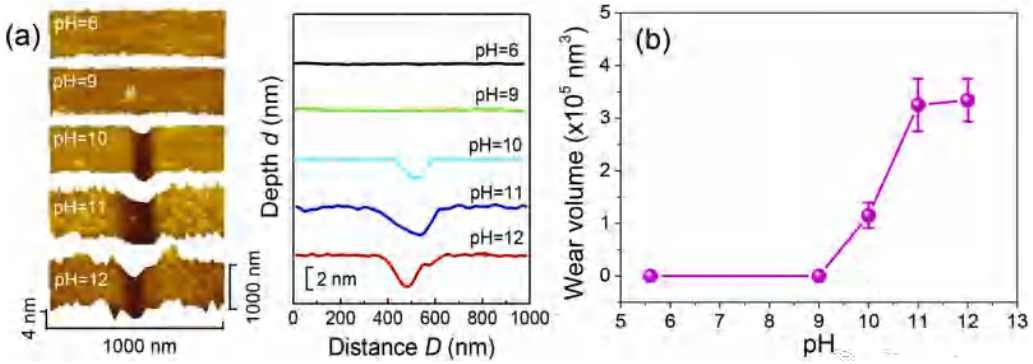

Fig. 2. Atomic removal of CaF_2 against SiO_2 microspherical tip at various pHs. (a) AFM images and corresponding cross-section profiles of the wear scars formed at various solution pHs at a normal load F_n of ~4.9 μN. (b) Wear volume on CaF_2 surfaces as a function of pH. The number of sliding cycle N is 200, sliding velocity v is 8 μm/s, and sliding distance D is 2 μm.

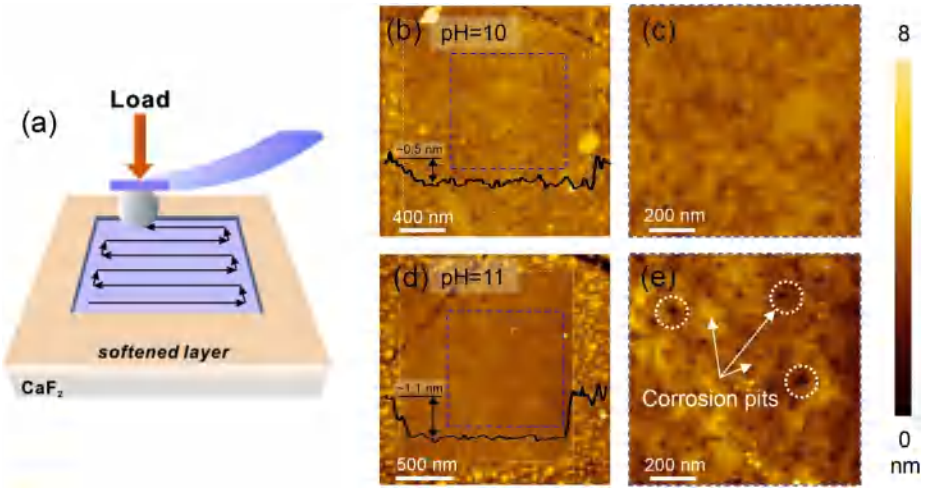

Fig. 3. Area scanning of CaF_2 surfaces against SiO_2 tip in KOH solutions at different pHs. (a) Schematic illustration of the area scanning of CaF_2 surface against a SiO_2 tip. (b) and (d) show the surface topography of CaF_2 surfaces after area scanning in KOH solution at pH = 10 and 11, respectively. (c) and (e) show the AFM images of the scanning regions marked by blue dotted line frames in (b) and (d), respectively. The normal load F_n is 4.9 μN, the number of sliding lines in a scanning area of 1.5 × 1.5 μm^2 is 512, and the sliding velocity v is 4 μm/s. (For interpretation of the references to colour in this figure legend, the reader is referred to the Web version of this article.)

of solution pH. As the number of sliding cycle increases, the friction force almost remains constant when no surface wear forms at pH ≤ 9. However, the friction force presents a gradual decrease at the initial sliding cycles as the atomic material removal occurs at pH > 9.

Comparison between the wear results in Fig. 2 and friction behaviors in Fig. 4 indicates that the increase in atomic material removal at higher pH does not result from mechanical interaction. To detect the tribochemical mechanism of CaF_2 in KOH solutions, the adhesive interactions between CaF_2/SiO_2 contact interfaces are compared under different pH conditions. In pure water with pH ≈ 6, the adhesion (pull-off) force is measured as ~0.5 μN (Fig. 5a). This value decreases to ~0.15 μN when the pH of the KOH solution increases to 11 (Fig. 5b). Notably, the adhesive interaction weakens when the tribochemical wear occurs at high pH. In contrast to the increase in the tribochemical wear of CaF_2 (Fig. 2), the adhesion force decreases gradually as the solution pH increases from 9 to 12 (Fig. 5c).

Fig. 6a compares the approach parts of the force-distance curves obtained at different solution pH values (red lines shown in Fig. 5a and b). The main contribution from van der Waals force results in the attractive interaction of two near-contacting surfaces [27], which is

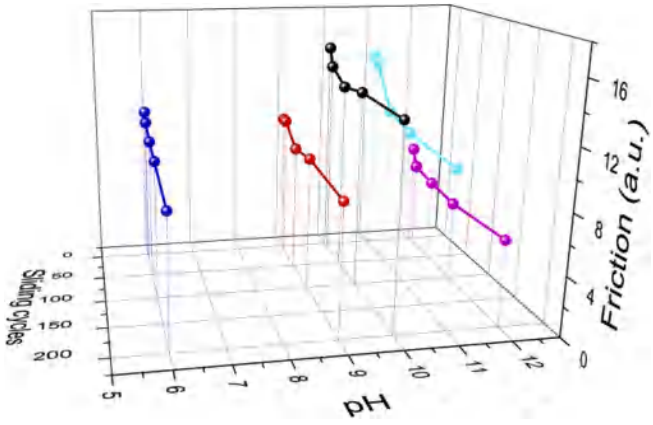

Fig. 4. Friction forces of CaF_2/SiO_2 interface as a function of the number of sliding cycles at different solution pHs. The applied normal load F_n is ~4.9 μN, and the sliding velocity v is 8 μm/s.

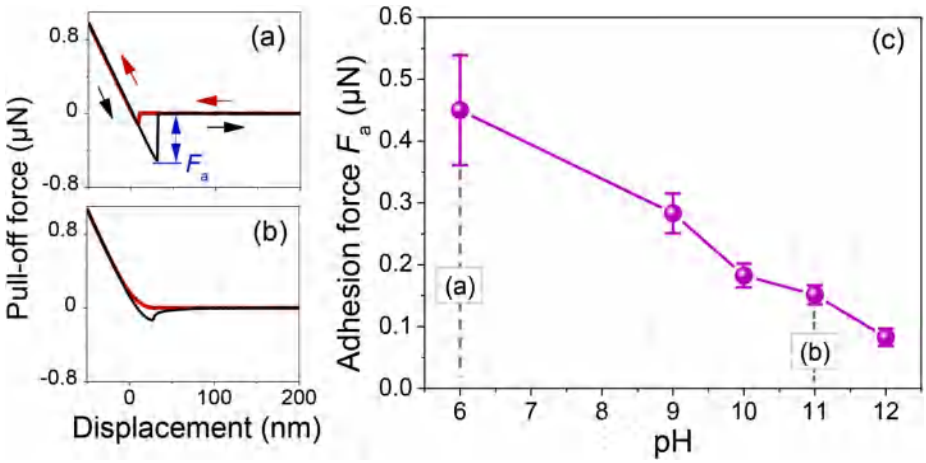

Fig. 5. Adhesion (pull-off) forces of CaF_2/SiO_2 interface at different solution pHs. (a) Force-distance curve obtained in pure water at pH = 6. F_a is the adhesion (pull-off) force. (b) Force-distance curve obtained in the KOH solution at pH = 11–12. Here, the red and black lines denote the approach and withdrawal between the CaF_2/SiO_2 contact surfaces, respectively. (c) Adhesion force of CaF_2/SiO_2 interface as a function of solution pH. (For interpretation of the references to colour in this figure legend, the reader is referred to the Web version of this article.)

indicated by the occurrence of a sudden jump as the AFM tip approaches. The jump force decreases markedly with the increase in solution pH, indicating that the attraction between the contacting interface continues to decline. In a liquid environment, the interfacial attraction should mainly come from van der Waals, bonding, and electrostatic forces [28]. Normally, van der Waals and bonding forces cause attraction of two contacting surfaces, and van der Waals force is slightly affected by the concentration of solution medium and pH [27]. Therefore, the variation in the attraction should be mainly attributed to the evolution of the electrical property of the contacting surfaces with solution pH.

The isoelectric point of silica is reported to be at pH = 2–5, above which the surface OH groups will ionize and lead to negative charges [29,30]. By comparison, the isoelectric point of CaF_2 crystal is approximately pH = 9 [31]. At pH < 9, the surface of CaF_2 will be positively charged because the outermost F^- dissolves faster than Ca^{2+} [31].

$$CaF_2 \Leftrightarrow CaF^+ + F^- \quad (1)$$

When pH > 9, F^- on the surface of CaF_2 begins to exchange with OH^- in KOH solution, and then $Ca(OH)_2$ softening layer is formed at the outermost surface [17].

$$CaF_2 + 2OH^- \Leftrightarrow Ca(OH)_2 + 2F^- \quad (2)$$

Under this condition, the positive charge on the surface of CaF_2 gradually disappears and possibly carries a small amount of negative charge due to the exchange of ion and the adsorption of OH groups [31]. The opposite charges of the CaF_2/SiO_2 contacting surfaces at pH < 9 correspond to an electrostatic attraction force. Then, the electrostatic and van der Waals forces overlap, causing a strong jump force as the SiO_2 tip approaches the CaF_2 surface (Fig. 6b). By contrast, the chemical reaction between CaF_2 and KOH at pH > 9 results in the same charges between CaF_2 and SiO_2 tip surfaces. When these two surfaces approach,

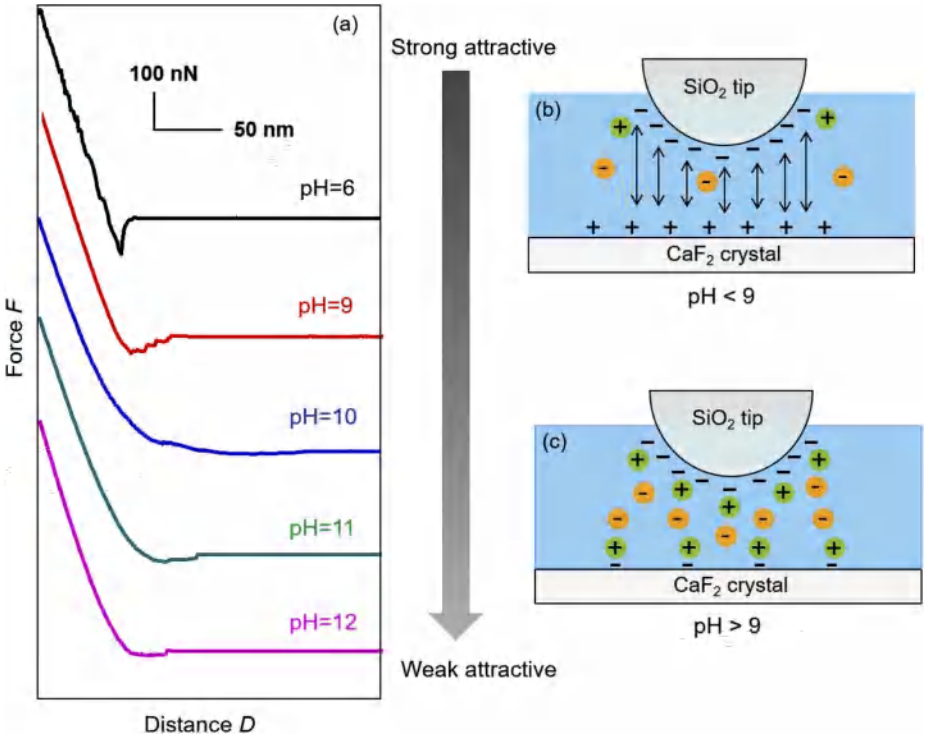

Fig. 6. (a) Approach parts of the force-distance curves of the CaF_2/SiO_2 contacting interface at different solution pH values. (b) and (c) illustrate the schematic diagrams of the interactions between CaF_2/SiO_2 contacting interface in pure water (pH = ~6) and in KOH solutions with different pH values (≥9), respectively.

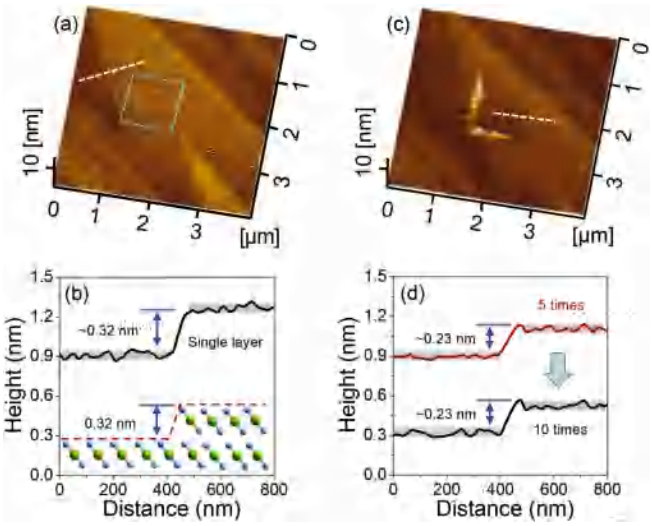

Fig. 7. Atomic layer removal of $CaF_2(111)$ sliding against a Si_3N_4 tip (radius ≈ 15 nm) after immersion for ~30 min in KOH solution at pH = 10. (a) AFM image of original $CaF_2(111)$ cleavage surface before KOH immersion after area scanning for five times in humid air (marked by azure dotted frame). (b) The cross-section profile of the atomic step is marked by white dotted lines in (a), and the atomic step height of the F–Ca–F single layer is ~0.32 nm (bottom schematic in b). (c) AFM image of the KOH-immersed $CaF_2(111)$ cleavage surface after area scanning for five times. (d) Comparison of the cross-section profiles of the wear area after scanning for 5 and 10 times (marked by white dotted lines in c). The scanning normal load F_n is 150 nN, the number of sliding lines inside the area-scanning region with 1 × 1 μm^2 is 512, and the sliding velocity v is 4 μm/s.

the force-displacement curves show long-range interaction as the electric double layers around the interface superimposing, and the electrostatic repulsion force will weaken the jump force in the force-displacement curves (Fig. 6c).

Previous studies reported that though the contact pressure was far less than the yield stress, some materials (i.e., silicon [19,32–34], gallium arsenide [35], and phosphate laser glass [36]) could be destroyed by the tribochemical reaction, that is, interfacial bond formation and breakage of substrate bonds, causing atomic material removal. Here, the increase in the repulsion force between the CaF_2/SiO_2 contacting surfaces with pH rising indicates that the material removal of CaF_2 in KOH solution is not due to the enhancement in interfacial interactions, such as adhesion or interfacial bond formation. Chemical corrosion with KOH solution (ion exchange) combined with the mechanical interaction acted by AFM tip should play a critical role in the tribochemical removal process of CaF_2.

3.3. Tribochemical removal mechanism of CaF_2 in KOH solution

To further detect the removal mechanism of CaF_2 in KOH solution, the atomic layer removal of $CaF_2(111)$ cleavage surface in humid air (RH ≈ 40%) is compared before and after immersion in KOH solution. A $CaF_2(111)$ cleavage surface with single F–Ca–F layer step (thickness ≈ 0.32 nm) is prepared firstly (Fig. 6a and b). Using area-scanning model (same as that shown in Fig. 3a), the atomic layer removal of the fresh $CaF_2(111)$ cleavage surface is studied by sliding against a Si_3N_4 tip (radius ≈ 15 nm) at a normal load of 150 nN in humid air. After repeating five sliding cycles, no marked surface damage can be observed (azure dotted frame in Fig. 7a). By contrast, atomic material removal with a depth of ~0.23 nm is formed on the KOH-solution-immersed $CaF_2(111)$ surface under the same area-scanning conditions (Fig. 7c and d). However, the wear depth does not change though another five scanning times are added (Fig. 7d), indicating that the value of ~0.23 nm is close to the thickness of the "softened layer" formed under the given pH conditions. These results support that the chemical reaction in Eq. (2) can result in the formation of Ca $(OH)_2$ "softened layer", which can be easily removed by AFM tip scratching. Surprisingly, the minimum removal depth (~0.23 nm) of $CaF_2(111)$ cleavage surface is close to the thickness of the Ca–F atomic layer (0.236 nm) [37]. Thus, we hypothesize that in the chemical reaction between $CaF_2(111)$ and KOH solution, only F^- at the outermost layer exchanges with OH^- in the KOH solution, and the internal F^- layer continues to bond with the substrate.

Fig. 8 shows the TEM observations of a wear scar on the CaF_2 surface formed in KOH solution at pH = 10. As shown in Fig. 8a and b, an approximately 5-nm-deep groove was formed on the CaF_2 surface after sliding a SiO_2 sphere under a contact pressure of 1.13 GPa. The high-resolution TEM image of the cross-section region (Fig. 8c) demonstrates perfect crystallographic lattice order in CaF_2 despite close proximity to the worn surface. Then, the occurrence of subsurface plastic deformation under this low contact pressure can be ruled out because no lattice defects (e.g., dislocation or slippage) are formed in the CaF_2 subsurface. Therefore, unlike the mechanical wear originating from amorphous transformation or crack initiation [38–40], the nondestructive material removal of CaF_2 in KOH should be mainly attributed to tribochemical reactions.

Fig. 9 schematically shows the tribochemical wear mechanism of CaF_2 in KOH solution. A pristine $CaF_2(111)$ surface is detected as fluorine terminated [41]. Chemically, the ionic exchange between OH^- in KOH solution and F^- on CaF_2 surface generates $Ca(OH)_2$ as an outermost "softened layer" [42,43]. The mechanical interaction applied by the SiO_2 tip during the sliding process can remove this softened layer at low contact pressure, resulting in surface wear. The decrease of friction force

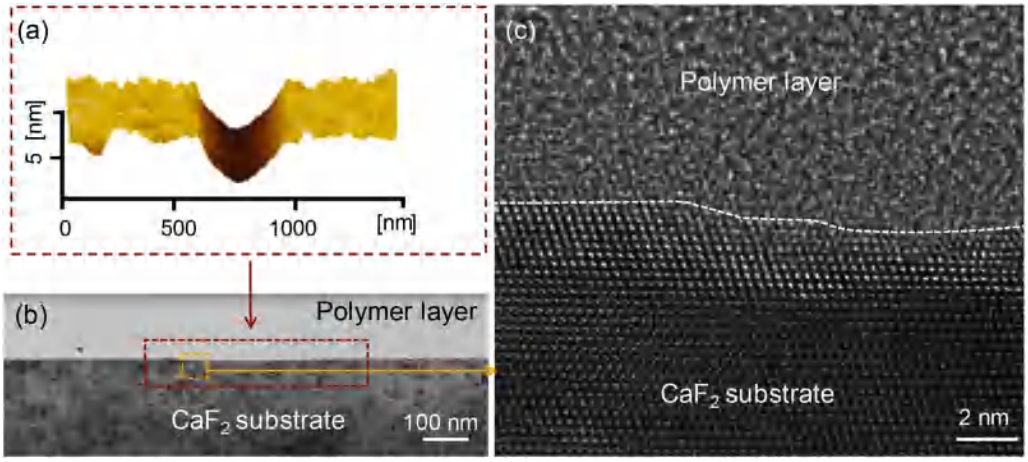

Fig. 8. TEM observations of the wear scar on the CaF_2 substrate formed in KOH solution at pH = 10. (a) AFM image showing an approximately 5-nm-deep wear scar formed on CaF_2 surface after sliding with a SiO_2 microsphere under the conditions of F_n = 4.9 μN, v = 40 μm/s, and sliding cycles N = 500. (b) TEM image of the cross-section of the wear scar. (c) Representative lattice-resolved image in the worn area marked with a box (yellow dotted line) in (b). (For interpretation of the references to colour in this figure legend, the reader is referred to the Web version of this article.)

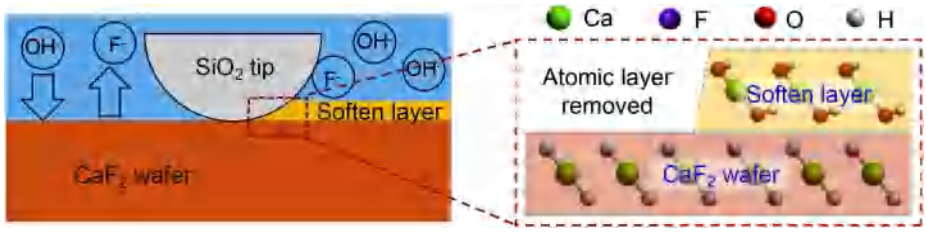

Fig. 9. Schematic illustration of the tribochemical wear of CaF_2 substrate slid against a SiO_2 tip in KOH solution. During the sliding process, the SiO_2 tip removes the formed softened layer (left picture), which is $Ca(OH)_2$ (right picture).

with sliding cycles at pH > 9 (Fig. 4) indicates that the mechanical or chemical properties of the softened layer may change along with the thickness direction due to the existence of native oxide layer or pre-reactively softened layer formed during handling process before nanowear tests. In addition, mechanical stress may lower the energy barrier for the initiation of chemical reaction [44] and facilitate the ion exchange between KOH solution and CaF_2 substrate. Then, the material removal of CaF_2 will be aggravated further. Given that minimal contact stress can only induce the elastic deformation of CaF_2 substrate, the crystallographic lattice of the substrate retains its original form after removal of the outermost surface softened layer (Fig. 8).

3.4. CMP of CaF_2(111) cleavage surface at the pH-optimized slurry

According to the AFM results, the optimized pH of KOH solution is 9–10, under which the material of CaF_2 can be removed at low contact stress and with minimized residual corrosion pits at the fabricated surface (Figs. 2 and 3). In actual CMP, the polishing pad drives the SiO_2 abrasive particles to attack the CaF_2 surface in rolling and sliding manners, causing the removal of surface softened layer [45]. During this process, the role of slurry pH is significant. The low pH of the CMP slurry will influence the polishing efficiency due to the weak chemical reaction and the agglomeration of SiO_2 abrasive particles [46]. However, extremely high pH may cause excessive chemical corrosion damage, lowering surface quality [26].

Here, the optimized pH condition obtained in the AFM tests is verified in the CMP of CaF_2 surface. A fresh CaF_2(111) cleavage surface is prepared by razor blade cleaving (Fig. 10a). This cleavage surface is first polished using a diamond abrasive in the pH-optimized slurry (pH = 9.5–10) to remove the atomic steps. Table 1 shows the polishing parameters. As shown in Fig. 10b, the CaF_2(111) surface with a RMS roughness of ~5 nm in 5 × 5 μm^2 is fabricated after the removal of surface atomic steps. Given the extreme high hardness of the diamond abrasives, scratch damage is unavoidable. Afterward, CMP with SiO_2 slurry is carried out at the optimized pH (9.5–10). Scratches on the CaF_2(111) surface can be completely removed, and surface roughness is finally reduced to ~0.37 nm (Fig. 10c). The fabrication of sub-nano rough surface without corrosion pit supports that the optimized pH condition obtained from AFM tests is effective in actual CMP of CaF_2.

4. Conclusions

The solution pH dependence of the tribochemical removal of CaF_2(111) against single SiO_2 abrasive was studied using AFM. The optimized pH for material removal occurring without residual corrosion wear at the fabricated surface was determined and verified in an actual CMP process. The main conclusions can be summarized as follows.

(1) Tribochemical wear of CaF_2(111) against single SiO_2 abrasive strongly depends on solution pH. The optimized pH of the solution for CaF_2 CMP is 9–10, below which no remarkable material was removed because the contact pressure was less than the material yield stress and above which the excessive chemical corrosion pits will be formed at the fabricated CaF_2(111) surface.

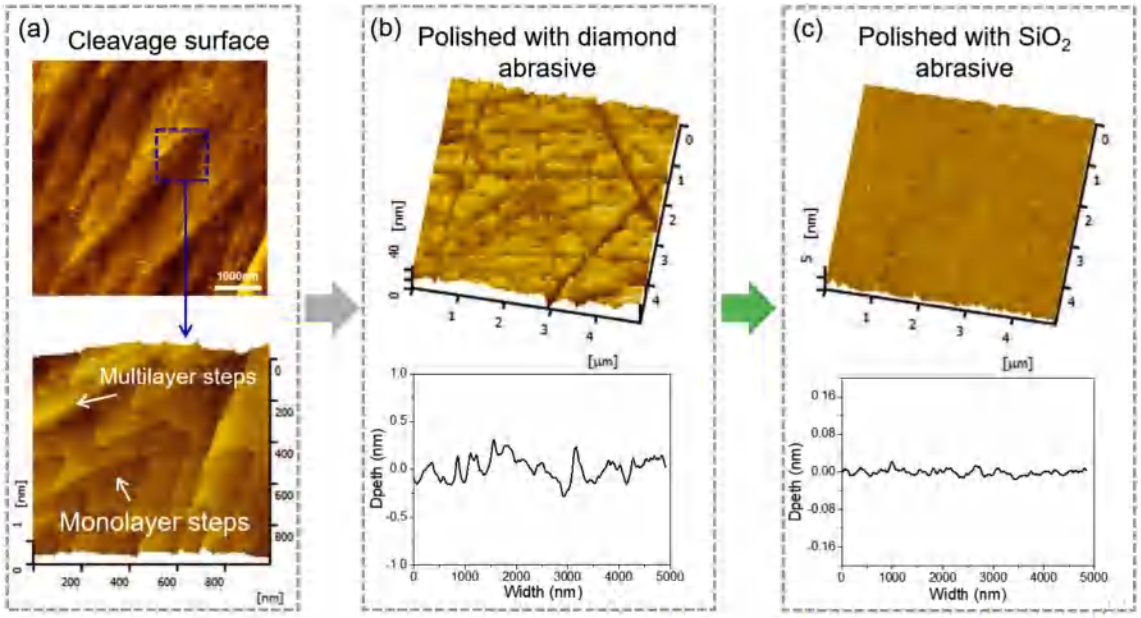

Fig. 10. CMP of CaF_2(111) cleavage surface in the slurry with the optimized pH (9.5–10). (a) AFM images of pristine CaF_2(111) cleavage surface. (b) AFM image and cross-section profile of the CaF_2(111) surface after polishing with diamond slurry. (c) AFM image and cross-section profile of CaF_2(111) surface after further polishing with SiO_2 slurry.

(2) In contrast to the increase in the tribochemical wear of CaF_2, the adhesive interaction between CaF_2/SiO_2 interface in KOH solution decreases gradually as solution pH rising. This result rules out the possibility that interfacial bond formation largely contributes to the tribochemical wear of CaF_2 in KOH solution.
(3) The material removal in humid air only occurring after corrosion in KOH solution and the perfect subsurface lattice detected by TEM observation support that the tribochemical wear of CaF_2 is mainly attributed to chemical corrosion combined with mechanical interaction. Based on this tribochemical reaction, the ultimate limit in polishing was demonstrated, that is, removal of $Ca–F^+$ layer from a CaF_2 cleavage surface. Meanwhile, the optimized pH of the slurry for polishing CaF_2(111) cleavage surface was applied in an actual CMP process and a sub-nano smooth CaF_2 surface without visible surface corrosion damage was fabricated under this condition.

Declaration of competing interest

The authors declare that they have no known competing financial interests or personal relationships that could have appeared to influence the work reported in this paper.

CRediT authorship contribution statement

Jie Guo: Investigation, Writing - original draft. **Jian Gong:** Investigation, Data curation, Formal analysis, Writing - original draft. **Pengfei Shi:** Data curation. **Chen Xiao:** Formal analysis. **Liang Jiang:** Resources. **Lei Chen:** Conceptualization, Writing - review & editing, Formal analysis, Funding acquisition, Supervision. **Linmao Qian:** Resources, Software, Supervision.

Acknowledgements

The authors are grateful for the financial support from the National Natural Science Foundation of China (51875486, 51991373) and Sichuan Science and Technology Program (2019YFH0098).

References

[1] Sils J, Hausfeld S, Clauß W, Pahl U, Lindner R, Reichling M. Impurities in synthetic fluorite for deep ultraviolet optical applications. J Appl Phys 2009;106:063109.
[2] Wagner C, Harned N. EUV lithography: lithography gets extreme. Nat Photon 2010;4:24–6.
[3] Enkisch H, Trenkler J. EUV lithography: technology for the semiconductor industry in 2010. EuroPhys News 2004;35:149–52.
[4] Li J, Liu YH, Dai YJ, Yue DC, Lu XC, Luo JB. Achievement of a near-perfect smooth silicon surface. Sci China-Technol Sci 2013;56:2847–53.
[5] Estragnat E, Tang G, Liang H, Jahanmir S, Pei P, Martin J. Experimental investigation on mechanisms of silicon chemical mechanical polishing. Electron. Mater. 2004;33:334–9.
[6] Johansen H, Kastner G. Surface quality and laser - damage behaviour of chemo - mechanically polished CaF_2 single crystals characterized by scanning electron microscopy. J Mater Sci 1998;33:3839–48.
[7] Rebecca SR, Robert S, Vincent PS. Effect of surface quality on transmission performance for (111) CaF_2. Appl Surf Sci 2001;183:264–9.
[8] Liang H. Chemical boundary lubrication in chemical-mechanical planarization. Tribol Int 2005;38:235–42.
[9] Namba Y, Ohnishi N, Yoshida S, Harada K, Yoshida K. Ultra-precision float polishing of calcium fluoride single crystals or deep ultra violet applications. CIRP annals 2004;53:459–62.
[10] Yin GJ, Li SY, Xie XH, Zhou L. Ultra-precision process of CaF_2 single crystal. Proceddings of SPIE 2014;6:9281.
[11] Lee H, Park Y, Lee S, Jeong H. Effect of wafer size on material removal rate and its distribution in chemical mechanical polishing of silicon dioxide film. Mech Sci Technol 2013;27:2911–6.
[12] Wang Y, Chen Y, Qi F, Xing Z, Liu W. A molecular-scale analytic model to evaluate material removal rate in chemical mechanical planarization considering the abrasive shape. Microelectron Eng 2015;134:54–9.
[13] Forsberg M. Effect of process parameters on material removal rate in chemical mechanical polishing of Si(100). Microelectron Eng 2005;77:319–26.
[14] Wang YG, Zhang LC, Biddut A. Chemical effect on the material removal rate in the CMP of silicon wafers. Wear 2011;270:312–6.
[15] Gotsmann B, Lantz MA. Atomistic wear in a single asperity sliding contact. Phys Rev Lett 2008;101:125501.
[16] Liu JJ, Notbohm JK, Carpick RW, Turner KT. Method for characterizing nanoscale wear of atomic force microscope tips. ACS Nano 2010;4:3763–72.
[17] Zhang P, Xiao C, Chen C, Chen L, Qian LM. Effect of abrasive particle size on tribochemical wear of monocrystalline silicon. Tribol Int 2017;109:222–8.
[18] Chen L, Wen JL, Zhang P, Yu BJ, Ma TB, Lu XC, Kim SH, Qian LM. Nanomanufacturing of silicon surface with a single atomic layer precision via mechanochemical reactions. Nat Commun 2018;9:1542.
[19] Chen C, Xiao C, Wang XD, Zhang P, Chen L, Qi YQ, Qian LM. Role of water in the tribochemical removal of bare silicon. Appl Surf Sci 2016;390:696–702.
[20] Barnette AL. Experimental and density functional theory study of the tribochemical wear behavior of SiO_2 in humid and alcohol vapor environments. Langmuir 2011;27:12702–8.
[21] Chen L, Hu LC, Xiao C, Qi YQ, Yu BJ, Qian LM. Effect of crystallographic orientation on mechanical removal of CaF_2. Wear 2017;376:409–16.
[22] Erickson C. Just scratching the surface: nanoscale wear on the fluorite (CaF_2) [111] cleavage plane. Washington State University, Ph.D. thesis; 2013.
[23] Gong J, Xiao C, Yu JX, Peng JF, Yu BJ, Chen L, Qian LM. Stress-enhanced dissolution and delamination wear of crystal CaF_2 in water condition. Wear 2019;418–419:86–93.
[24] Dickinson JT, Park NS, Kim MW, Langford SC. A scanning force microscope study of a tribochemical system: stress-enhanced dissolution. Tribol Lett 1997;3:69–80.
[25] Torii A, Sasaki M, Hane K, Okuma S. A method for determining the spring constant of cantilevers for atomic force microscopy. Meas Sci Technol 1996;7:179–84.
[26] Estragnat E, Tang G, Liang H, Jahanmir S, Pei P, Martin J. Experimental investigation on mechanisms of silicon chemical mechanical polishing. J Electron Mater 2004;33:334–9.
[27] Israelachvili JN. Intermolecular and surface forces. New York: Elsevier INC press; 2012.
[28] Xiao XD, Qian LM. Investigation of humidity-dependent capillary force. Langmuir 2000;16:8153–8.
[29] Lis D, Backus EHG, Hunger J, Parekh SH, Bonn M. Liquid flow along a solid surface reversibly alters interfacial chemistry. Science 2014;6188:344.
[30] Cui XG, Zin WC, Cho WJ, Ha CS. Nonionic triblock copolymer synthesis of SBA-15 above the isoelectric point of silica (pH = 2–5). Mater Lett 2005;59:2257–61.
[31] Becraft KA, Richmond GL. In situ vibrational spectroscopic studies of the CaF_2/H_2O interface. Langmuir 2001;17:7721–4.
[32] Chen L, He H, Wang X, Kim SH, Qian LM. Tribology of Si/SiO_2 in humid air: transition from severe chemical wear to wearless behavior at nanoscale. Langmuir 2015;31:149–56.
[33] Chen L, Kim SH, Wang X, Qian LM. Running-in process of $Si\text{-}SiO_x/SiO_2$ pair at nanoscale-sharp drops in friction and wear rate during initial cycles. Friction 2013;1:81–91.
[34] Jacobs TDB, Carpick RW. Nanoscale wear as a stress-assisted chemical reaction. Nat Nanotechnol 2013;8:108–12.
[35] Yu BJ, Gao J, Jin CN, Xiao C, Wu J, Liu HY, Jiang SL, Chen L, Qian LM. Humidity effects on tribochemical removal of GaAs surfaces. APEX 2016;9:066703.
[36] Yu J, He H, Zhang Y, Hu H. Nanoscale mechanochemical wear of phosphate laser glass against a CeO_2 particle in humid air. Appl Surf Sci 2017;392:523–30.
[37] Zhurova EA, Maksimov BA, Simonov VI, Sobolev BP. Structural studies of CaF_2 (at 296 K) and $Ca_{1-x}Pr_xF_{2+x}$ (at 296 and 170 K) crystals with x=0.1: the changes in the fluorite anionic motif in the partial substitution of Ca^{2+} by Pr^{3+} cations. Crystallogr Rep 1996;41:438–43.
[38] Zarudi I, D Cheong WC, Zou J, Zhang LC. Atomistic structure of monocrystalline silicon in surface nano-modification. Nanotechnology 2004;15:104–7.
[39] Ribeiro R, Shan Z, Minor AM, Liang H. In situ observation of nano-abrasive wear. Wear 2007;263:1556–9.
[40] Liu ZH, Gong J, Xiao C, Shi PF, Kim SH, Chen L, Qian LM. Temperature-dependent mechanochemical wear of silicon in water: the role of Si-OH surfacial groups. Langmuir 2019;35:7735–43.
[41] Giessibl FJ, Reichling M. Investigating atomic details of the CaF_2(111) surface with a qplus sensor. Nanotechnology 2005;16:S118–24.
[42] Leeuw NHD, Cooper TG. A computational study of the surface structure and reactivity of calcium fluoride. J Mater Chem 2003;13:93–101.
[43] Khatib R, Backus EHG, Bonn M, Perez-Haro M, Gaigeot M, Sulpizi M. Water orientation and hydrogen-bond structure at the fluorite/water interface. Sci Rep 2016;6:24287.
[44] Jacobs TDB, Gotsmann B, Lantz MA, Carpick RW. On the application of transition state theory to atomic-scale wear. Tribol Lett 2010;39:257–71.
[45] Zhao D, Lu X. Chemical mechanical polishing: theory and experiment. Friction 2013;1:306–26.
[46] Pietsch GJ, Higashi GS, Chabal YJ. Chemomechanical polishing of silicon: surface termination and mechanism of removal. Appl Phys Lett 1994;64:3115–7.